supporting materials

# Tuning Electronic Structure of Phosphonic Acid-based Deep Eutectic Solvents for Synergistically Catalytic Oxidative Desulfurization

Lixian Xu, [a] Jie Yin, [a] Dongao Zhu, [a] Beibei Zhang, [b] Linhua Zhu, [c] Hongping Li, [a] Jing He, [a] Huaming Li [a] and Wei Jiang*[a]

[a] Institute for Energy Research, Jiangsu University, Zhenjiang 212013, P. R. China.

[b] College of Chemistry and Chemical Engineering, Yancheng Institute of Technology, Yancheng 224061, P. R. China.

[c] College of Chemistry and Chemical Engineering, Key Laboratory of Water Pollution Treatment and Resource Reuse of Hainan Province, Hainan Normal University, Haikou 571158, P.R. China.

E-mail: jiangwei@ujs.edu.cn

# Experimental

## Materials

Phenylphosphinic acid (PIA), phenylphosphonic acid (POA), zinc chloride ($ZnCl_2$, 98%), aqueous hydrogen peroxide ($H_2O_2$, 30wt%), carbon tetrachloride ($CCl_4$), tertbutyl alcohol (TBA) and benzoquinone (BQ), dodecane ($C_{12}H_{26}$, 99%) and hexadecane ($C_{16}H_{34}$, 98%) was Shanghai Aladdin Biochemical Technology Co., Ltd. Dibenzothiophene (DBT, 98%), 4-methyldibenzothiophene (4-MDBT, 96%) and 4,6-dimethyldibenzothiophene (4,6-DMDBT, 97%) were obtained from Merck KGaA. These chemicals can be used directly due to their analytical grade purity.

## Desulfurization procedure

The different model oils comprising 200, 500, 800 and 1000 mg $kg^{-1}$ dibenzothiophene (DBT) in n-dodecane with tetradecane as internal standard were prepared to investigate desulfurization performance of PDES. Except the DBT, 4-MDBT and 4,6-DMDBT were also selected as the heterocyclic sulphides in model oil to simulate the environment of real diesel fuel. The mass of the material to be weighed is calculated by the following formula. Formula (1) is to calculate the mass of sulfide DBT, where $M_{(sulfide)}$ is the relative molecular mass of sulfide, $C_{(sulfide)}$ is the concentration of sulfide in fuel oil, $M_{(S)}$ is the relative mass of S atom, which is 32 g/mol, formula (2) is to calculate the mass of internal standard substance n-hexadecane, and formula (2) is to calculate the mass of solvent n-dodecane.

$$m_{(sulfide)} = m_{(oil)} \times M_{(sulfide)} \times C_{(sulfide)} / (M_{(s)} \times \text{wt.\%}_{(\text{ sulfide})}) \quad (1)$$

$$m_{(standard)} = m_{(oil)} \times C_{(standard)} / \text{wt.\%}_{(standard)} \quad (2)$$

$$m_{(\mathrm{oil})} \approx \rho_{(\mathrm{oil})} \times V_{(\mathrm{oil})} \quad (3)$$

Among them, $\rho$(n-dodecane) = 0.753 g/cm$^{-3}$. The relative molecular weights of sulfides (DBT, 4-MDBT 4,6-DMDBT) were 184.26 g/mol, 198.28 g/mol, 212.31 g/mol, respectively.

Internal standard method was used to detect the concentration of sulfide in model oil by gas chromatography (Shimadzu, GC-2010 plus). The model of capillary column was SH-RTx-5 (30 m× 0.25 mm × 0.25 μm) and the detector is hydrogen flame ionization detector (FID). When the model oil is dodecane and the internal standard is hexadecane, the procedure of GC column incubator is as follows:

(1) For the model oil with DBT as substrate, the initial column temperature was set at 100 $^{\mathrm{o}}$C, the injection port temperature was set at 250 $^{\mathrm{o}}$C, and the temperature of GC-FID detector was set at 300 $^{\mathrm{o}}$C. The running time of DBT in GC is 5.89 min.

(2) Analysis of model oil with 4-MDBT as substrate: the setting program is the same as that with DBT as substrate, but the running time of 4-MDBT in GC is 6.45 min.

(3) For the model oil with 4,6-DMDBT as the substrate, the initial column temperature was set at 100 $^{\mathrm{o}}$C, the injection port temperature was set at 250 $^{\mathrm{o}}$C, the temperature was raised to 160 $^{\mathrm{o}}$C at the rate of 30 $^{\mathrm{o}}$C/min, and then to 250 $^{\mathrm{o}}$C at the rate of 35 $^{\mathrm{o}}$C/min, and the temperature of GC-FID detector was set at 300 $^{\mathrm{o}}$C. The running time of 4,6-DMDBT in GC is 6.44 min.

The typical desulfurization experiment was operated at 45 °C. In general, 0.5 g of PDES $ZnCl_2$/2PIA and 5 mL of prepared model fuels were added into a customized reaction vessel. Firstly, the mixed system was stirred for 30 min to investigate the extraction desulfurization ability of bifunctional PDES. Then, 9.6 μL of $H_2O_2$ (30 wt%) was injected into the system and sulfur content in the oil phase after reaction was periodically analysed by gas chromatography equipped with a flame ionization detector. The sulfur removal and Nernst partition coefficient ($K_N$) in PDES-ECODS reaction system are calculated by Eq. 1 and Eq. 2, in which $C_0$ is the original sulfur content in the model oil and $C_t$ is the sulfur content after reaction over a period of time (t min).

$$\text{sulfur removal}(\%) = \frac{C_0 - C_t}{C_0} \times 100 \tag{1}$$

$$K_N = \frac{\text{mg(sulfur removal)g}^{-1}\text{(DESs)}}{\text{mg(sulfur removal)g}^{-1}\text{(oil)}} \tag{2}$$

After the reaction, the model oil, which was sulfur-free, and the used PDES separated into two phases within the PDES-ECODS system. The upper oil phase was removed by decantation. The used PDES phase was then extracted with 5 mL of carbon tetrachloride ($CCl_4$) at room temperature for 10 min. The extracted layer was analyzed using gas chromatography-mass spectrometer (GC-MS) spectroscopy to qualitatively assess the types of products. In the recycling experiment, the clean fuel was removed after the reaction, and no further operations were performed on the used PDES. Fresh fuel and oxidant were sequentially added for subsequent runs until the sulfur removal efficiency significantly decreased. The experimental conditions remained consistent across each cycle. Naphthalene and indole were added to simulate the actual fuel environment and further evaluate the resistance of the PDES to interference from aromatic hydrocarbons and nitrogen-containing compounds.

## Mutual solubility of the PDES and the model oil

The solvent of all prepared and used model oils is n-dodecane. 1 g PDES and 5 mL n-dodecane were put into the reaction device and stirred the liquid mixture with a constant speed of 600 r/min at 45 $^{o}$C for 30 min. After full contact between PDES and n-dodecane, let the liquid mixture stand for a while to phase equilibrium. Then, the structure of PDES and n-dodecane after mixing were characterized by FT-IR and $^1$H NMR, respectively, and compared with the primitive PDES and n-dodecane.

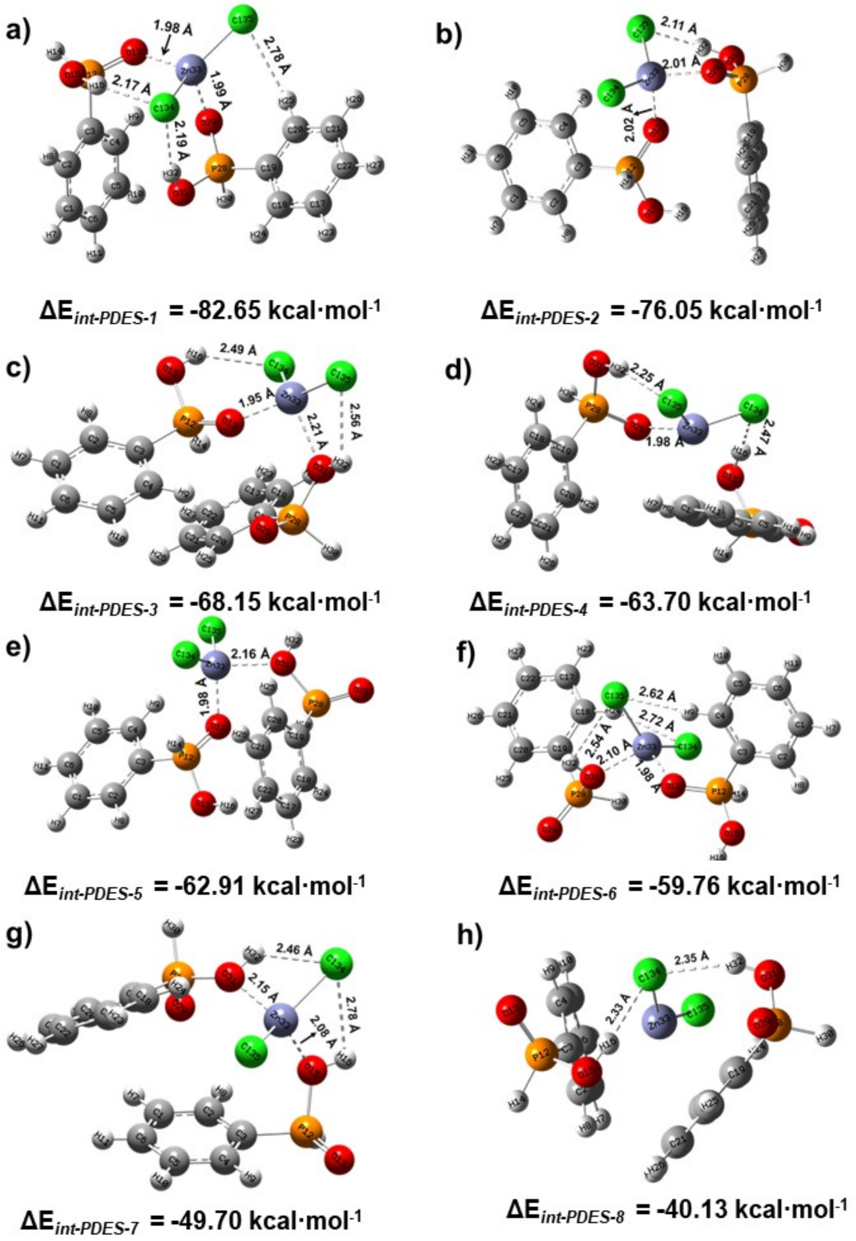

$\Delta E_{int\text{-}PDES\text{-}1}$ = -82.65 kcal·mol$^{-1}$ $\Delta E_{int\text{-}PDES\text{-}2}$ = -76.05 kcal·mol$^{-1}$

$\Delta E_{int\text{-}PDES\text{-}3}$ = -68.15 kcal·mol$^{-1}$ $\Delta E_{int\text{-}PDES\text{-}4}$ = -63.70 kcal·mol$^{-1}$

$\Delta E_{int\text{-}PDES\text{-}5}$ = -62.91 kcal·mol$^{-1}$ $\Delta E_{int\text{-}PDES\text{-}6}$ = -59.76 kcal·mol$^{-1}$

$\Delta E_{int\text{-}PDES\text{-}7}$ = -49.70 kcal·mol$^{-1}$ $\Delta E_{int\text{-}PDES\text{-}8}$ = -40.13 kcal·mol$^{-1}$

Fig. S1. Optimized configurations of PDES $ZnCl_2$/2PIA: a) PDES-1, b) PDES-2, c) PDES-3, d) PDES-4, e) PDES-5, f) PDES-6, g) PDES-7 and h) PDES-8.

Table S1. Desulfurization performance of raw materials

| Entry | Raw materials | EDS [a] | ECODS [b] |
|---|---|---|---|
| | | Sulfur removal/% | |
| 1 | $ZnCl_2$ | 1.8 | 4.8 |
| 2 | PIA | 2.4 | 3.4 |

| | | | |
|---|---|---|---|
| 3 | PA | 1.4 | 6.2 |
| 4 | POA | 2.7 | 4.1 |

Reaction conditions: m (raw material) = 1 g, V(model fuel) = 5 mL, T = 45 $^{o}$C. $^{a}$ t = 15 min. $^{b}$ O/S = 3, t = 45 min.

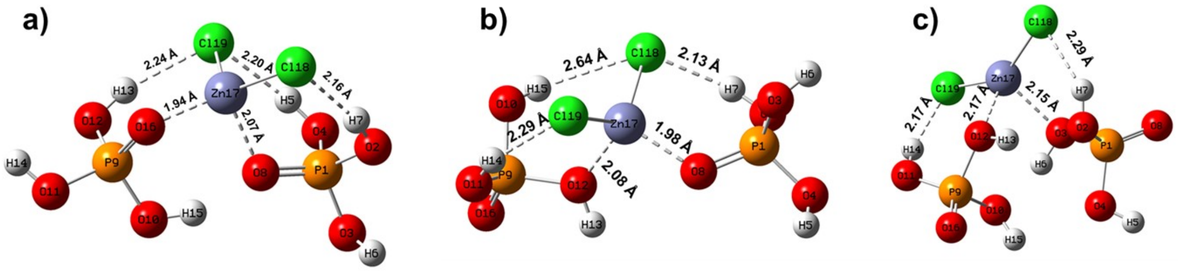

E$_{int}$ = -91.46 kcal·mol$^{-1}$ E$_{int}$ = -71.22 kcal·mol$^{-1}$ E$_{int}$ = -64.02 kcal·mol$^{-1}$

Fig. S2. Optimized configurations of ZnCl$_2$/2PA.

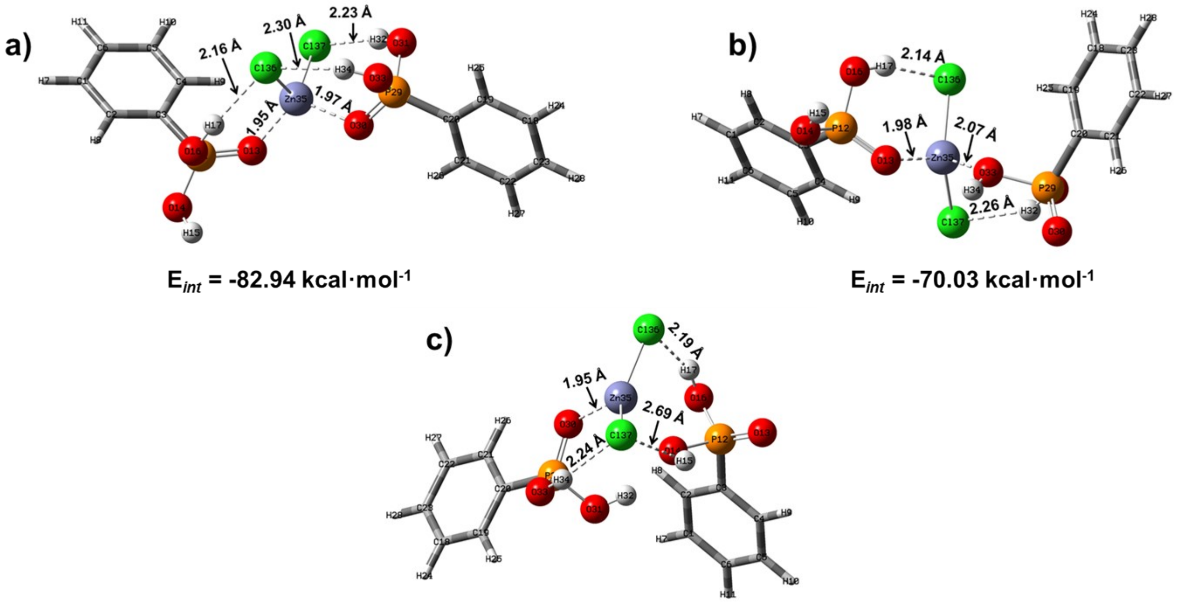

E$_{int}$ = -82.94 kcal·mol$^{-1}$ E$_{int}$ = -70.03 kcal·mol$^{-1}$

E$_{int}$ = -38.31 kcal·mol$^{-1}$

Fig. S3. Optimized configurations of ZnCl$_2$/2POA.

Table S2. The natural bond orbital (NBO) charge of Zn atom and O atom of P=O and the bond order of Zn···O in different catalysts.

| Catalyst | $q_{Zn}$ | $q_o$ on P=O | | The bond order of Zn···O | |
|---|---|---|---|---|---|
| PA | - | -1.063 | | | |
| PIA | - | -1.062 | | | |
| POA | - | -1.075 | | | |
| $ZnCl_2$ | 1.061 | | | | |
| $ZnCl_2$/2PA | 1.077 | O16(-1.120) | O8(-1.154) | O16…Zn17 (0.291) | O8…Zn17 (0.302) |
| $ZnCl_2$/2PIA | 1.101 | O29(-1.082) | O13(-1.104) | O13…Zn33 (0.269) | O29…Zn33 (0.254) |
| $ZnCl_2$/2POA | 1.095 | O30(-1.110) | O13(-1.122) | O13…Zn35 (0.274) | O30…Zn35 (0.283) |

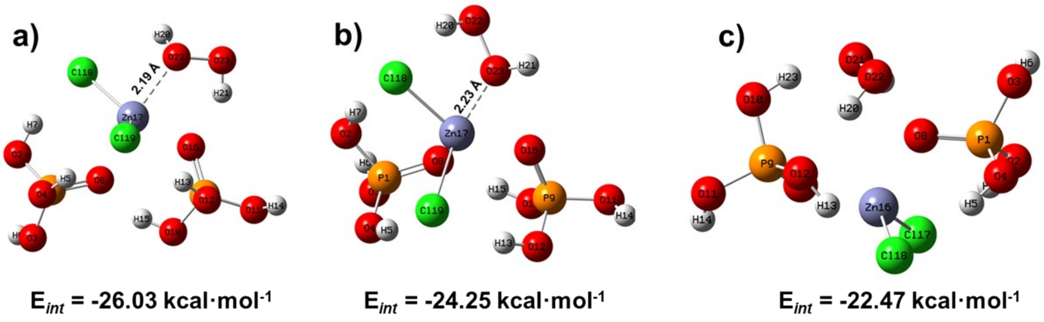

$E_{int}$ = -26.03 kcal·mol$^{-1}$ $E_{int}$ = -24.25 kcal·mol$^{-1}$ $E_{int}$ = -22.47 kcal·mol$^{-1}$

Fig. S4. Optimized configurations for $ZnCl_2$/2PA and $H_2O_2$.

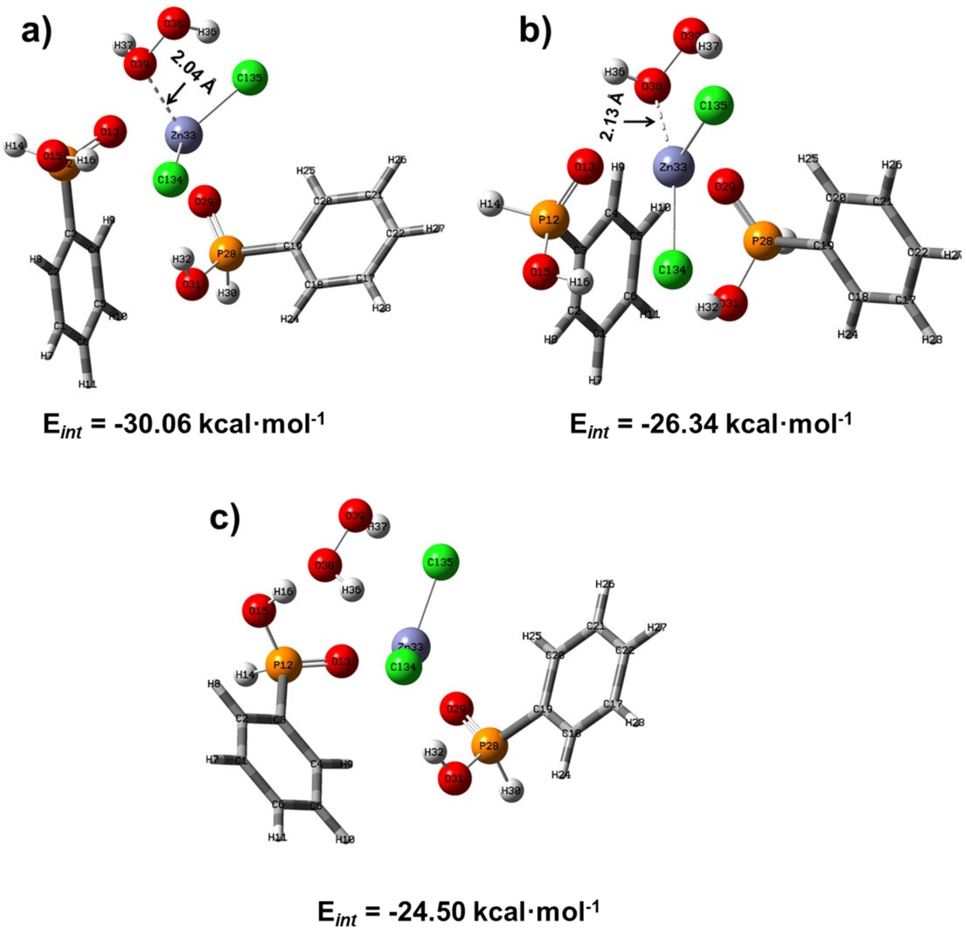

$E_{int}$ = -30.06 kcal·mol$^{-1}$

$E_{int}$ = -26.34 kcal·mol$^{-1}$

$E_{int}$ = -24.50 kcal·mol$^{-1}$

Fig. S5. Optimized configurations for $ZnCl_2$/2PIA and $H_2O_2$.

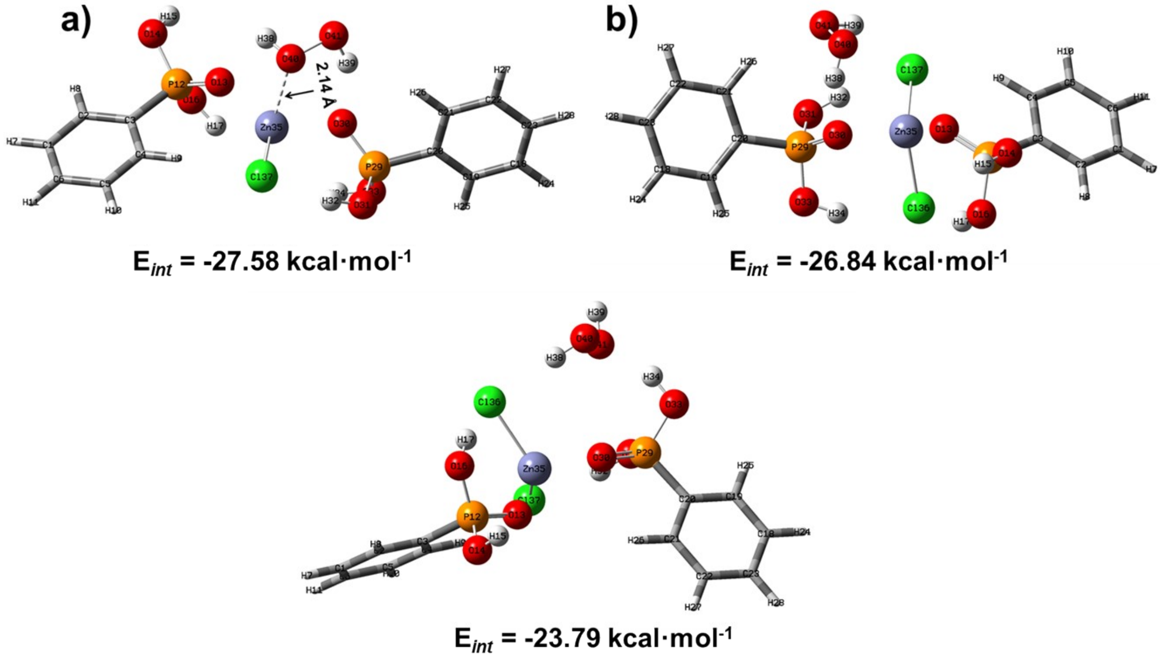

$E_{int}$ = -27.58 kcal·mol$^{-1}$

$E_{int}$ = -26.84 kcal·mol$^{-1}$

$E_{int}$ = -23.79 kcal·mol$^{-1}$

Fig. S6. Optimized configurations for $ZnCl_2$/2POA and $H_2O_2$.

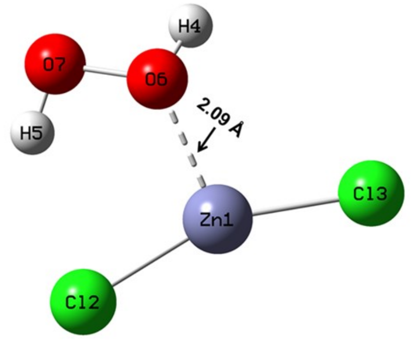

$E_{int}$ = -15.78 kcal·mol$^{-1}$

Fig. S7. Optimized configurations for $ZnCl_2$ and $H_2O_2$.

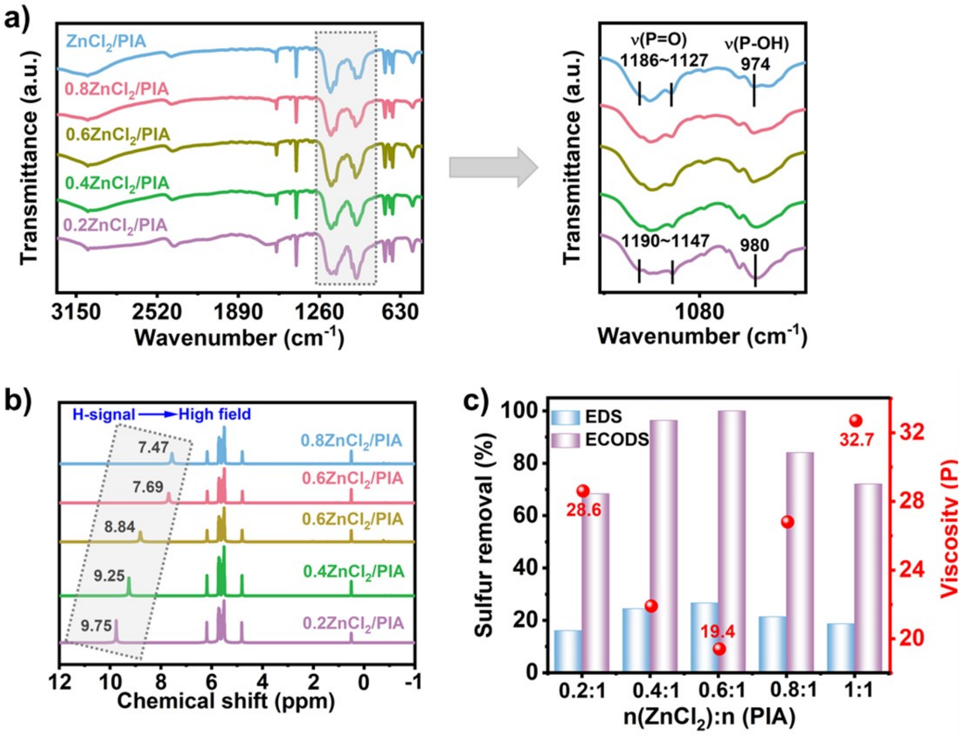

Fig. S8. The FT-IR (a) and 1H NMR (b) spectra of PDESs ($xZnCl_2/PIA$, x = 0.2, 0.4, 0.6, 0.8, 1). (c) Effect of viscosity on desulfurization at different $ZnCl_2$ concentration. Reaction conditions: m (PDES) = 1.0 g, V (model fuel containing DBT, 200 $mg.kg^{-1}$) = 5 mL, T = 45 $^oC$, O/S = 3, t = 30 min. The test temperature of viscosity for PDES is 45 $^oC$.

The detailed analysis that additional experiments using PDESs with varying $ZnCl_2/PIA$ molar ratios (x = 0.2, 0.4, 0.6, 0.8, 1), combined with spectroscopic analysis and catalytic performance tests, to provide deeper insights into $ZnCl_2$'s role in oxidative desulfurization in Fig. S8 is as follows:

## 1. $ZnCl_2$ modulates the electronic structure of PDES via coordination interactions

### (1) FT-IR analysis

As the $ZnCl_2$ ratio increases (x = 0.2→1), the stretching vibration peak of the P=O bond in PIA (1192 ~1149 $cm^{-1}$ ) gradually shifts to lower wavenumbers (1186~1127 $cm^{-1}$), and the P–OH vibration peak (984 $cm^{-1}$ ) shifts to 974 $cm^{-1}$ (Fig. S8a). This confirms that $ZnCl_2$ forms stable P=O···Zn coordination bonds with the P=O group of PIA, reducing the electron density of the P=O bond and increasing its bond length[1, 2]. Coordination interactions further enhance the charge density of $Zn^{2+}$, thereby strengthening its interaction with $H_2O_2$.

### (2) $^1H$ NMR analysis

The active hydrogen signal (-POOH) in PIA shifts upfield (9.75 ppm→7.47 ppm) as the $ZnCl_2$ ratio increases, with peak narrowing (Fig. S8b). This indicates:

**Hydrogen bond reorganization**: $ZnCl_2$ forms -OH···Cl hydrogen bonds with PIA's -

OH group, disrupting PIA's intrinsic hydrogen-bonding network and exposing more active sites[3, 4].

**Electronic redistribution**: Coordination interactions redistribute electron density in PIA, enhancing $Zn^{2+}$'s Lewis acidity and promoting $H_2O_2$ adsorption/activation.

### 2. $ZnCl_2$ ratio governs catalytic performance

Desulfurization efficiency exhibits a volcano-type trend with $ZnCl_2$ ratio (x): optimal performance occurs at x = 0.6 (100% sulfur removal), while lower (x = 0.2, 67.8%) or higher (x = 1, 42.6%) ratios reduce activity (Fig S8c). This aligns with viscosity data (lowest viscosity at x = 0.6: 11.7 P), suggesting:

- **Optimal coordination structure**: At x = 0.6, $ZnCl_2$ and PIA form a stable coordination complex, maximizing $Zn^{2+}$'s electronic regulation capacity.
- **Enhanced mass transfer**: Low viscosity (11.7 P) facilitates reactant (DBT, $H_2O_2$) diffusion within the PDES phase, improving reaction kinetics.

### 3. $ZnCl_2$'s dual role in oxidant activation

Theoretical calculations and determination of reactive oxygen species (original Fig. 2c and Fig. 6 in manuscript) reveal $Zn^{2+}$'s coordination environment activates $H_2O_2$ via:

- **Enhanced $H_2O_2$ adsorption**: Increased $Zn^{2+}$ charge density raises adsorption energy ($\Delta E = 30.06\ \mathrm{kcal \cdot mol^{-1}}$).
- **Reactive oxygen species generation**: The $Zn^{2+}$–OOH intermediate undergoes homolytic cleavage to produce •OH and $\bullet O_2^-$ radicals (ESR detects DMPO-$O_2^-$ and DMPO-HO• signals), directly oxidizing DBT to $DBTO_2$
- **Synergistic acid catalysis**: Brønsted acid sites (–POOH) and Lewis acid sites

($Zn^{2+}$ ) cooperatively promote $H_2O_2$ heterolysis, forming reactive PDES-OOH peracid ($^1H$ NMR: 8.67 ppm→6.45 ppm).

**Conclusion**

$ZnCl_2$ in PDES regulates $Zn^{2+}$'s electronic structure via coordination, optimizing $H_2O_2$ adsorption/activation while forming a low-viscosity system for efficient mass transfer. Supplemental data validate $ZnCl_2$'s dual role (electronic modulation and mass transfer enhancement), advancing mechanistic understanding.

## UV-Vis acidity evaluation

The preparation of the solution is carried out in a glove box with a water content below 1 ppm. All spectra were recorded using a Perkin-Elmer spectrophotometer. During the recording process, the PDES is kept closed under argon gas to prevent any contamination during the experiment. The calculation formula for the Hamiltonian function ($H_0$) is as follows:

$$H_0 = pK(I)aq + \log([I]/[IH^+])$$

Wherein, $pK(I)_{aq}$ refers to the pKa value of the indicator in aqueous solution, and $[IH^+]$ and $[I]$ are the molar concentrations of the protonated and unprotonated forms of the indicator in the solvent, respectively.

Table S3. Calculation and comparison of Hammett functions for different DESs

| Entry | PDESs | $A_{max}$ | [ln]/% | $[lnH^+]$/% | $H_0$ |
|---|---|---|---|---|---|
| 1 | 4-nitroaniline | 1.05 | 100 | 0 | - |
| 1 | $ZnCl_2$/2PIA | 0.61 | 58.1 | 41.9 | 1.13 |
| 2 | $ZnCl_2$/2POA | 0.93 | 88.6 | 11.4 | 1.88 |

Indicator: 4-nitroaniline ($pK(I)_{aq} = 0.99$).

## The experimental design of operating parameters on desulfurization

Table S4. Screening parameters and designated levels in the desulfurization process.

| Entry | Parameters | levels | | | |
|---|---|---|---|---|---|
| 1 | Temperature (°C) | 30 | 35 | 40 | 45 |
| 2 | The dosage of DES (g) | 0.25 | 0.5 | 0.75 | 1 |
| 3 | Oxidant to sulfur molar ratio (O/S) | 2 | 2.5 | 3 | 3.5 |

Table S5. $L_9(3^4)$ orthogonal array experiment designed for the optimization of desulfurization factors.

| Entry | Temperature (°C) | The dosage of DES (g) | O/S | Sulfur-removal (%) |
|---|---|---|---|---|
| 1 | 30 | 0.25 | 2 | 42.4 |
| 2 | 30 | 0.5 | 2.5 | 52.3 |
| 3 | 30 | 0.75 | 3 | 61.1 |
| 4 | 30 | 1 | 3.5 | 89.7 |
| 5 | 35 | 0.25 | 2.5 | 68.8 |
| 6 | 35 | 0.5 | 2 | 78.1 |
| 7 | 35 | 0.75 | 3.5 | 99.9 |
| 8 | 35 | 1 | 3 | 99.9 |
| 9 | 40 | 0.25 | 3 | 76.7 |
| 10 | 40 | 0.5 | 3.5 | 94.7 |

| | | | | |
|---|---|---|---|---|
| 11 | 40 | 0.75 | 2 | 99.9 |
| 12 | 40 | 1 | 2.5 | 99.9 |
| 13 | 45 | 0.25 | 3.5 | 82.1 |
| 14 | 45 | 0.5 | 3 | 98.7 |
| 15 | 45 | 0.75 | 2.5 | 99.9 |
| 16 | 45 | 1 | 2 | 99.9 |

Table S6. Analysis results of variance and range for the optimization of desulfurization factors.

| Entry | Parameters | Partial $\eta^2$ | F-value | P-value | R |
|---|---|---|---|---|---|
| 1 | Temperature (°C) | 0.528 | 4.471 | 0.025 | 33.78 |
| 2 | The dosage of DES (g) | 0.365 | 2.297 | 0.130 | 29.85 |
| 3 | O/S | 0.064 | 0.274 | 0.843 | 11.52 |

*The criteria for determining the significance between each factor and desulfurization is $P<0.05$. The smaller the P value, the stronger the factor significance probability. R represents the range value of each factor. The greater the R value, the more obvious the interference of the parameter.

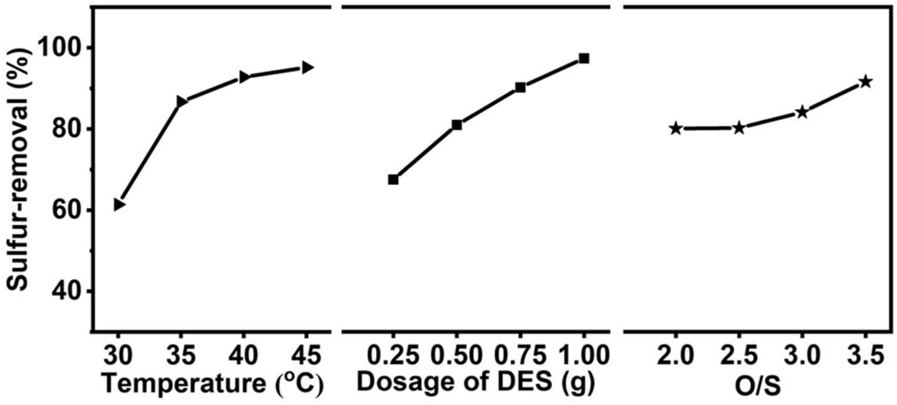

Fig. S9. Comparison of variance analysis between various factors and sulfur removal.

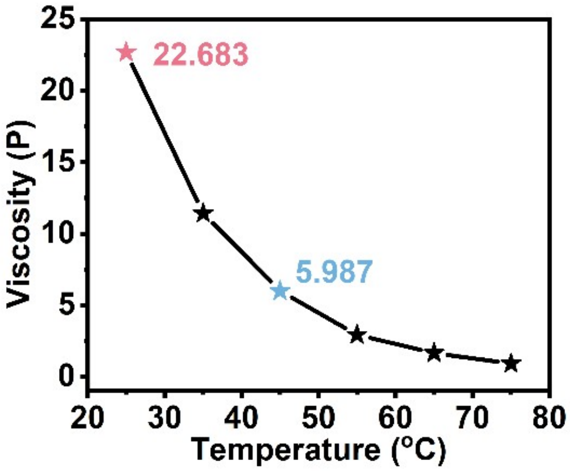

Fig. S10. Trend of viscosity changes with temperature in PDES $ZnCl_2$/2PIA.

## Reaction kinetics analysis of PDES-ECODS

For a more in-depth study of the relationship between desulfurization efficiency and reaction temperature, the kinetics research of the oxidative reaction was carried out. As shown in Fig. S11a, the reaction was in accord with the pseudo-first-order kinetics as follows:

$$ln\frac{Co}{Ct} = kt \tag{1}$$

where $C_0$ (ppm) is the total sulfur concentration and $C_t$ (ppm) is the sulfur concentration at certain reaction time t,and k is the first-order rate constant ($min^{-1}$). It could be observed that the constant k increased from 0.027 to 0.169 $min^{-1}$ when the temperature raised from 25 to 65 °C, which indicates the acceleration of reaction along with the increasing of reaction temperature.

According to the Arrhenius equation:

$$-\ln k = \frac{Ea}{RT} - \ln A \tag{2}$$

the apparent activation energy for the current oxidation of DBT was estimated to be 34.3 kJ mol$^{-1}$, as is shown in Fig. S11b.

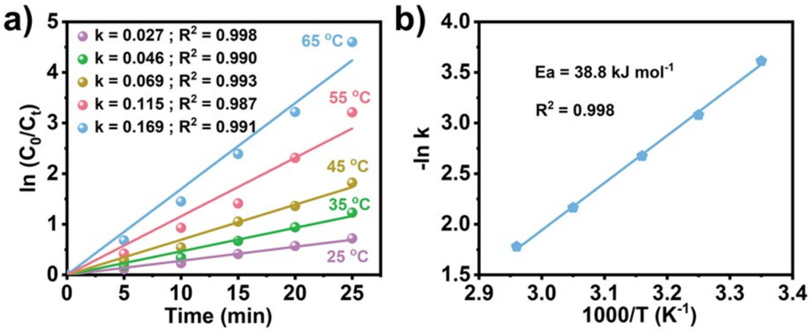

Fig. S11. a) Pseudo-first-order kinetics for the oxidative of DBT under different reaction. b) Activation energy for DBT oxidation reaction. Reaction conditions: m (PDES) = 1.0 g, V (model fuel containing DBT, 200 mg.kg$^{-1}$) = 5 mL, O/S = 3.

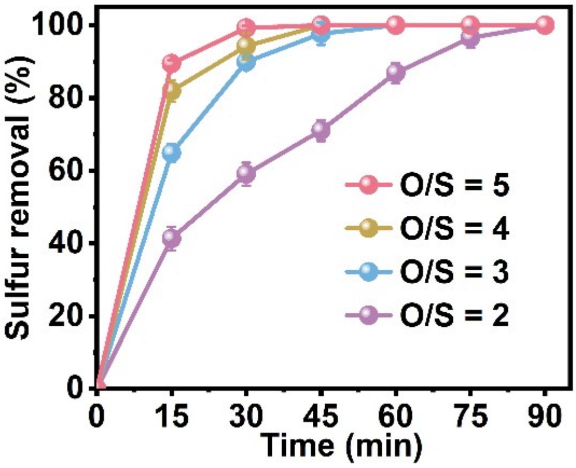

Fig. S12. Effect of added amount of oxidant on sulfur removal. Reaction conditions: m (PDES) = 1.0 g, V (model fuel containing DBT, 200 mg.kg$^{-1}$) = 5 mL, T = 45 $^{o}$C.

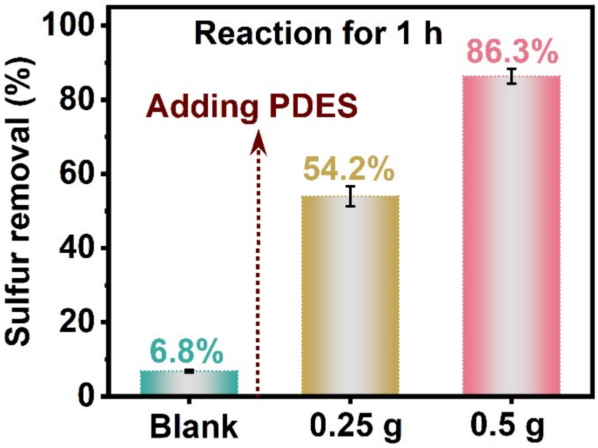

Fig. S13. Comparison of desulfurization with and without PDES $ZnCl_2$/2PIA in oxidation reactions. Reaction conditions: V (model fuel containing DBT, 200 mg.kg$^{-1}$) = 5 mL, T = 45 $^oC$, O/S = 3.

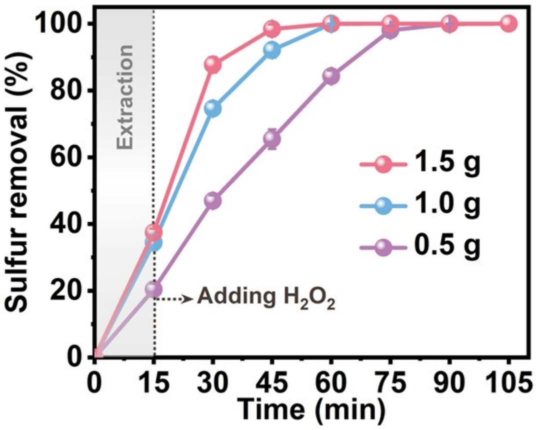

Fig. S14. Optimization of PDES dosage on sulfur removal. Reaction conditions: V (model fuel containing DBT, 200 mg.kg$^{-1}$) = 5 mL, T = 45 $^oC$, O/S = 3.

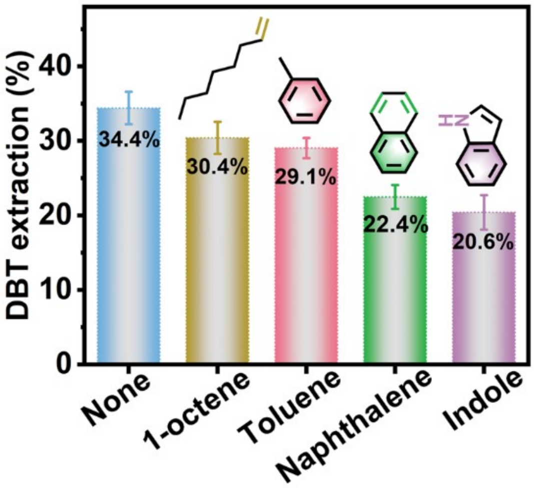

Fig. S15. Effect of interfering agents on extracting DBT. Reaction conditions: m (PDES) = 1.0 g, V (model fuel containing DBT, 200 mg.kg$^{-1}$) = 5 mL, T = 45 $^{o}$C, w (interfering agents) = 10 wt %.

To further investigate the extraction of aromatic sulfides over the PDES $ZnCl_2$/2PIA, aromatics, olefins, polycyclic aromatic hydrocarbons and aromatic nitrides, such as toluene, 1-octene, naphthalene and indoles, were added into reaction system. It was found from Fig. S15 that the mass transfer process of sulfide was seriously hindered and the extraction of DBT significantly reduced when there was aromatic ring structure in interfering agents. This might be caused by the affinity competitive of extraction reaction between interfering agents and PDES, which would also affect the subsequent catalytic oxidation process.

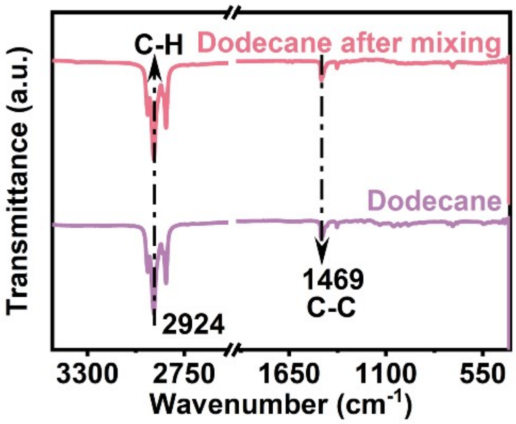

Fig. S16. FT-IR spectra of dodecane and dodecane after mixing with PDES $ZnCl_2$/2PIA.

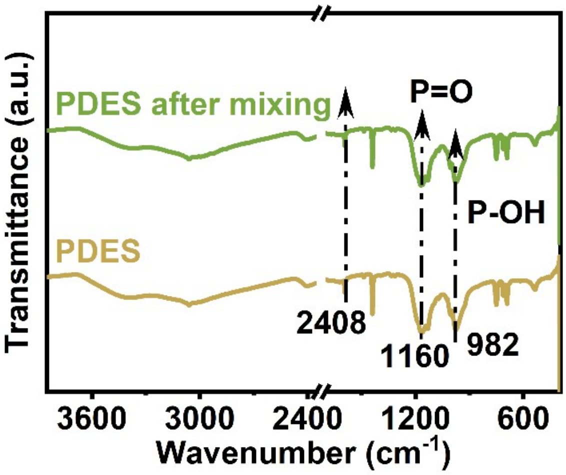

Fig. S17. FT-IR spectra of PDES $ZnCl_2$/2PIA and PDES after mixing with dodecane.

Through spectral analysis of PDES and dodecane solvent in fuel before and after mixing, it was found in Fig. S16 and Fig. S17 that the structure of PDES and dodecane remains unchanged, illustrating that PDES and fuel were not miscible.

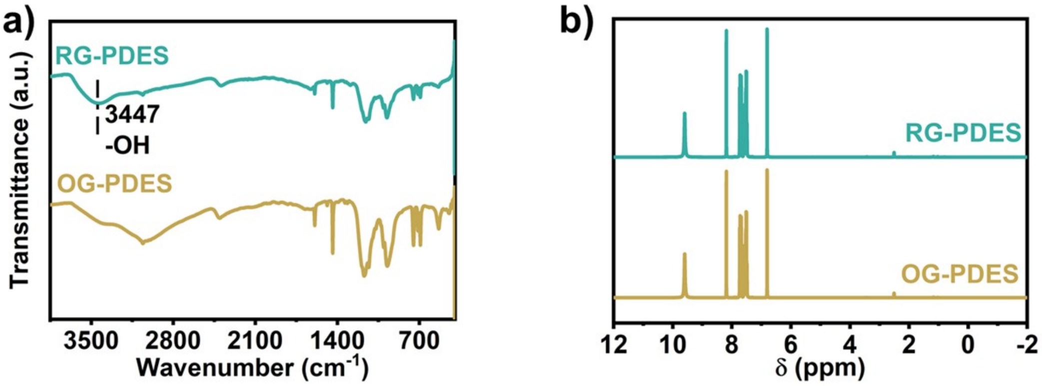

Fig. S18. (a) FT-IR and (b) $^1$H NMR spectra of original DES (OG-DES) and regenerated DES (RG-DES). Deuterated chloroform ($CDCl_3$) as reagent.

Table S7. Comparison of DBT removal performance in different catalyst-ODS systems.

| Entry | Catalyst (Extractant) | Reaction conditions | Sulfur removal (%) | Recycle times | Ref. |
|---|---|---|---|---|---|
| 1 | $ZnCl_2$/2PIA (1.0 g) | V(Oil) = 5 mL, T = 45 °C, O/S = 3, t = 45 min | 100 | 11 | This work |
| 2 | $C_5HNO\cdot 0.3FeCl_3$ (1.0 g) | V(Oil) = 5 mL, T = 30 °C, O/S = 12, t = 180 min | 97 | 6 | [5] |
| 3 | $[Bmim][HSO_4]$ (2.5 g) | V(Oil) = 5 mL, T = 50 °C, O/S = 5, t = 90 min | 85.5 | 6 | [6] |
| 4 | $[ODBU]Cl/3ZnCl_2$ (1 g) | V(Oil) = 5 mL, T = 50 °C, O/S = 6, t = 120 min | 99 | 3 | [7] |
| 5 | $[Hnmp]Cl/3ZnCl_2$ (1.0 g) | V(Oil) = 5 mL, T = 75 °C, O/S = 8, t = 20 min | 98.7 | 4 | [8] |
| 5 | $[C_2(MIM)_2]PW_{12}O_{40}$ (0.2 g) | V(Oil) = 5 mL, T = 60 °C, O/S = 6, t = 60 min | 98.4 | 7 | [9] |
| 6 | $[C_2(MIM)_2]_2VW_{12}O_{40}$ (0.02 g) | V(Oil) = 5 mL, T = 60 °C, O/S = 5, t = 20 min | 100 | 5 | [10] |
| 7 | $[C_4ImBS][PW_{12}O_{40}]$ (0.5 g) | V(Oil) = 5 mL, T = 60 °C, O/S = 6, t = 60 min | 100 | 3 | [11] |

| | | | | | |
|---|---|---|---|---|---|
| 8 | YS-Vo-NMO<br>([BMIM]$BF_4$, 1 mL) | V(Oil) = 5 mL, T = 60 °C, O/S = 5 | 99.5 | 9 | 12 |
| 9 | Na-$MoO_3$/SBA-15<br>(acetonitrile, 10 mL) | V(Oil) = 10 mL, T = 60 °C, O/S = 8 | 94.0 | 5 | 13 |
| 11 | $Mo_{12}O_{40}$/KIT-6<br>(acetonitrile, 20 mL) | V(Oil) = 20 mL, T = 60 °C, O/S = 5 | 100 | 9 | 14 |
| 12 | MOF-808<br>(MeCN, 2 mL) | V(Oil) = 2 mL, T = 50 °C, O/S = 5 | 100 | 8 | 15 |
| 13 | Ti-UiO-66<br>(acetonitrile, 10 g) | V(Oil) = 10 g, T = 60 °C, O/S = 6 | 91.7 | 3 | 16 |

To systematically evaluate the catalytic performance of the PDES $ZnCl_2$/2PIA, a comparative comparison was conducted with traditional oxidative desulfurization systems employing ionic liquids or metal oxysalts as catalysts (Table S7). Compared to ionic liquids, PDES $ZnCl_2$/2PIA as catalyst exhibit significant catalytic advantages and superior reusability for oxidative desulfurization (ODS) in mild reaction conditions. Specifically, PDESs maintained 98.4% desulfurization efficiency after 12 consecutive cycles, far exceeding the performance of ionic liquids based ODS systems (typically ≤6 cycles). This enhanced recyclability stems from the robust coordination interactions within PDES (e.g., Zn···P=O bonds), which prevent metal leaching and structural degradation. In contrast to metal oxide catalysts, which often require additional organic extractants (e.g., acetonitrile) and harsh conditions (e.g., high O/S ratios or elevated temperatures), bifunctional PDESs enable solvent-free, ultradeep desulfurization under mild conditions (45°C, O/S = 3). For instance, conventional metal oxides like $MoO_x/TiO_2$ or MOFs achieved full desulfurization only with excessive oxidant (O/S = 4 ~ 8) and volatile co-solvents, raising environmental and economic concerns. These comparisons highlight PDESs as a sustainable, high-performance alternative to traditional ODS catalysts. Their unique dual functionality (extractant and catalyst), energy-efficient operation, and exceptional stability align with green chemistry principles, offering a scalable pathway for producing ultraclean fuels.

**Operation of using GC-MS to determine oxidation product**

The oxidation product was determined by GC-MS analysis to further understand the extraction coupling catalytic oxidation desulfurization process as shown in Fig S19 and Fig 4b. Take 1 g PDES $ZnCl_2$/2PIA and 5 mL model oil containing DBT with initial sulfur content of 200 ppm and put them into the reaction vessel. The reaction was stirred at 45 ℃ for 15 min. After standing for 1 min, DES phase and oil phase appeared delamination. The upper layer was oil phase and the lower layer was PDES phase. Take 1 uL of the upper oil phase and measure its residual sulfur content by GC, and the remaining 127.21327 ppm (the extractive desulfurization rate was 36.4%). Other conditions remained unchanged, 9.6 uL $H_2O_2$ (30 wt%) was added to the reaction system, and the reaction was stirred for 45 min. After standing for 1 min, residual sulfur content of the upper oil phase was measured by GC, and the remaining 0.01622 ppm (the oxidative desulfurization rate was 100%). In order to confirm the structure of the oxidation product, the PDES phase containing the oxidation product and oxidation product in the lower layer was extracted with $CCl_4$ solvent. Take 1 g reacted PDES and 5mL $CCl_4$ into the reaction vessel and stir at room temperature for 30 min. The oxidation products and oxidation product are soluble in $CCl_4$, but PDES is not. The

$CCl_4$ phase was detected by GC-MS. By m/z analysis, the oxidation product was dibenzothiophene sulfone ($DBTO_2$).

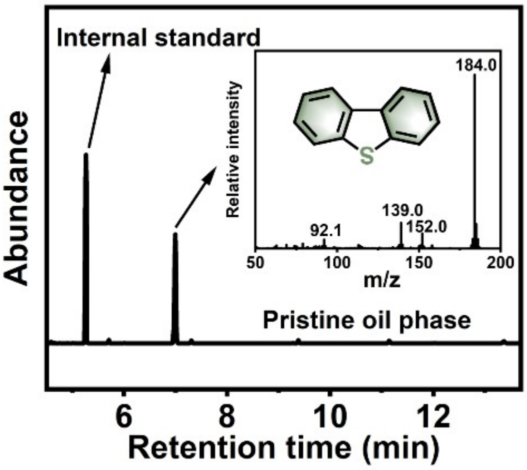

Fig. S19. The GC–MS of main compounds of the pristine oil phase.

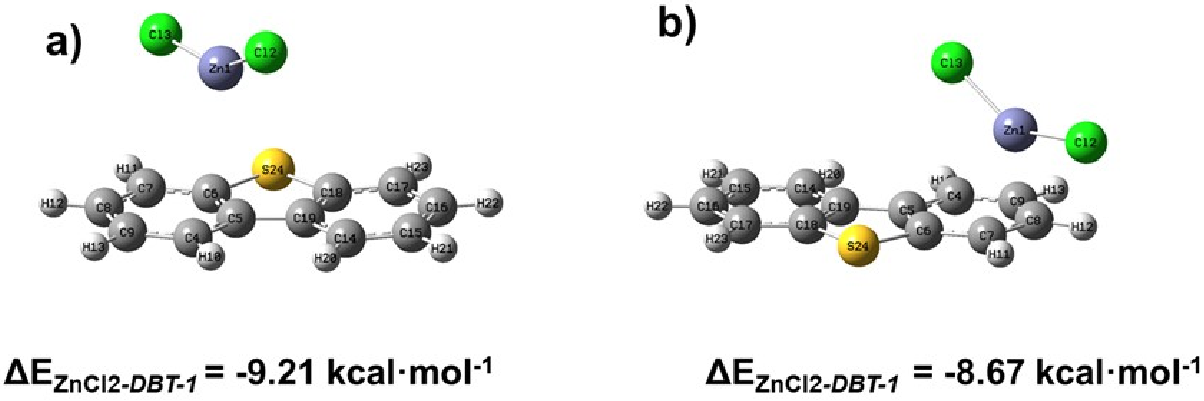

Fig. S20. Optimized configurations for $ZnCl_2$ and DBT complexes.

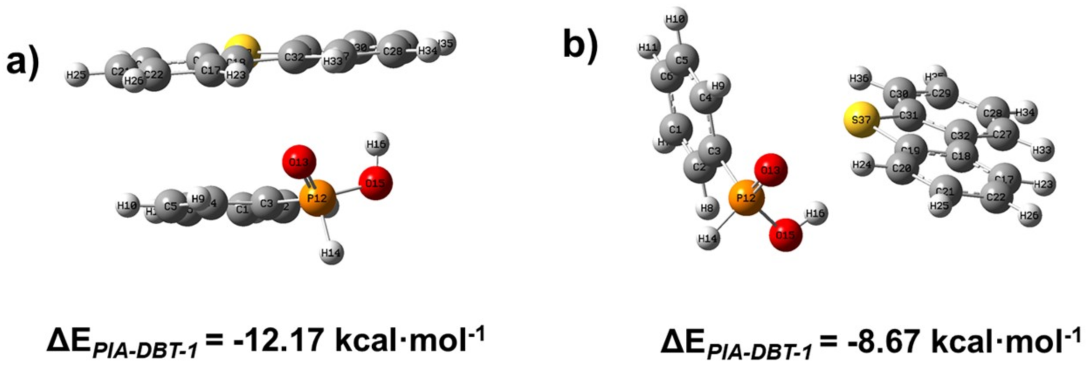

$\Delta E_{PIA\text{-}DBT\text{-}1}$ = -12.17 kcal·mol$^{-1}$

$\Delta E_{PIA\text{-}DBT\text{-}1}$ = -8.67 kcal·mol$^{-1}$

Fig. S21. Optimized configurations for PIA and DBT.

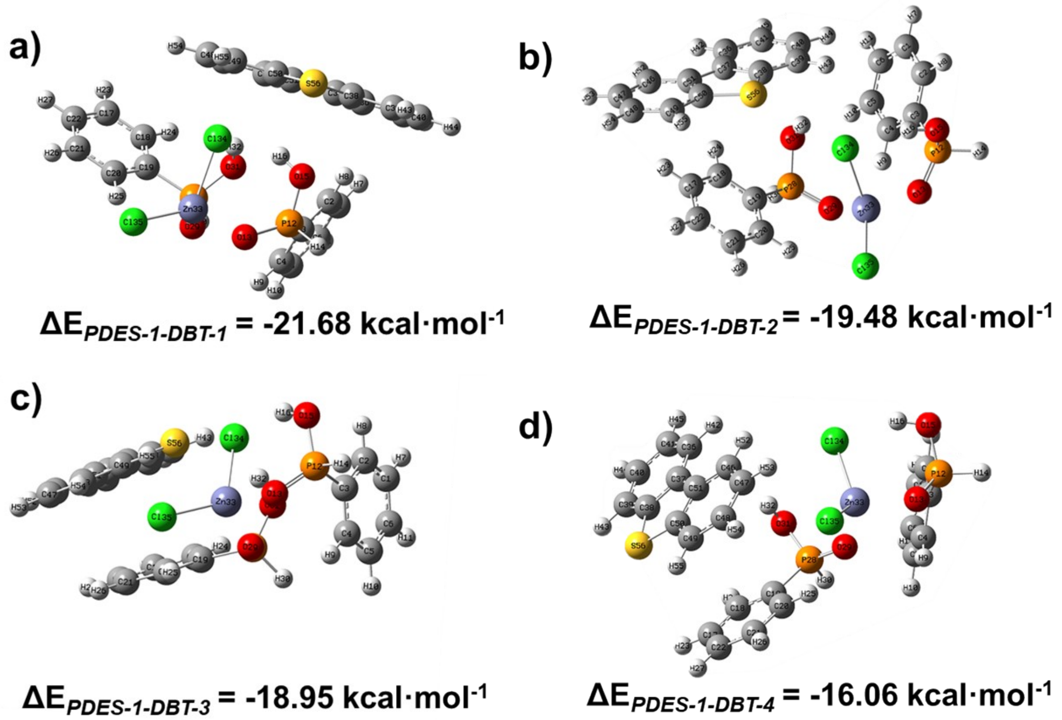

$\Delta E_{PDES\text{-}1\text{-}DBT\text{-}1}$ = -21.68 kcal·mol$^{-1}$

$\Delta E_{PDES\text{-}1\text{-}DBT\text{-}2}$ = -19.48 kcal·mol$^{-1}$

$\Delta E_{PDES\text{-}1\text{-}DBT\text{-}3}$ = -18.95 kcal·mol$^{-1}$

$\Delta E_{PDES\text{-}1\text{-}DBT\text{-}4}$ = -16.06 kcal·mol$^{-1}$

Fig. S22. Optimized configurations for PDES-1 and DBT.

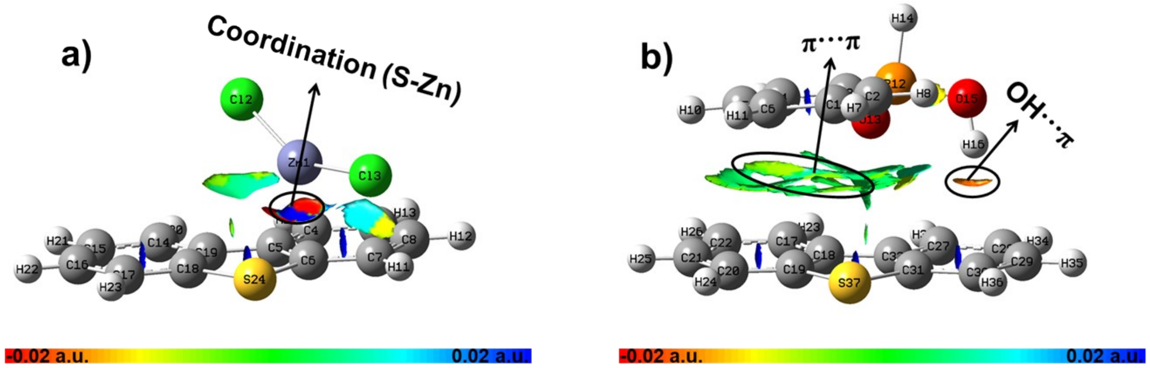

Fig. S23. Gradient isosurfaces (s=0.35 a.u.) for the optimized structure (a) $ZnCl_2$-DBT-1 and (b) PIA-DBT-1.

## References

1 H. Wang, S. Liu, Y. Zhao, J. Wang, Z. Yu, *ACS Sustainable Chem. Eng.,* **2019**, *7*, 7760-7767.

2 R. Saputra, R. Walvekar, M. Khalid, N. M. Mubarak, *J. Mol. Liq.,* **2020**, *310*, 113232.

3 L. Zhang, J. Wang, Y. Sun, B. Jiang, H. Yang, *Chem. Eng. J.,* **2017**, *328*, 445-453.

4 H. Yang, B. Jiang, Y. Sun, L. Hao, Z. Huang, L. Zhang, *Chem. Eng. J.,* **2016**, *306*, 131-138.

5 F.-t. Li, B. Wu, R.-h. Liu, X.-j. Wang, L.-j. Chen, D.-s. Zhao, *Chem. Eng. J.,* **2015**, *274*, 192-199.

6 H. Gao, C. Guo, J. Xing, J. Zhao, H. Liu, *Green Chem.,* **2010**, *12*, 1220-1224.

7 J. Wang, L. Zhang, Y. Sun, B. Jiang, Y. Chen, X. Gao, H. Yang, *Fuel Process. Technol.,* **2018**, *177*, 81-88.

8 X. Chen, H. Guo, A. A. Abdeltawab, Y. Guan, S. S. Al-Deyab, G. Yu, L. Yu, *Energy Fuels,* **2015**, *29*, 2998-3003.

9 X.-X. Xing, H.-L. Guo, T.-M. He, X. An, H.-P. Li, W.-S. Zhu, H.-M. Li, J.-Y. Pang, D.-B. Dang, Y. Bai, *ACS Sustain. Chem. Eng.,* **2022**, *10*, 11533-11543.

10 J. Li, Y. Guo, J. Tan, B. Hu, *Catalysts,* **2021**, *11*, 11030356.

11 Q. Wu, Q. Shi, J. Shang, M. Wang, H. Li, D. Shi, Y. Zhao, Q. Jiao, *ACS Omega,* **2020**, *5*, 31171-31179.

12 X. An, L. Xu, L. Xu, L. Zhu, J. She, J. He, W. Jiang, W. Zhu, H. Li, *Inorg. Chem.,* **2023**, *62*, 9199-9208.

13 Y. Tu, T. Li, G. Yu, L. Wei, L. Ta, Z. Zhou, Z. Ren, *Energ. Fuel.,* **2019**, *33*, 8503-8510.

14 Y. Ding, J. Wang, M. Liao, J. Li, L. Zhang, J. Guo, H. Wu, *Chem. Eng. J.,* **2021**,

*418*, 129470.

15 H. Q. Zheng, Y. N. Zeng, J. Chen, R. G. Lin, W. E. Zhuang, R. Cao, Z. J. Lin, *Inorg. Chem.,* **2019**, *58*, 6983-6992.

16 G. Ye, H. Qi, X. Li, K. Leng, Y. Sun, W. Xu, *ChemPhysChem,* **2017**, *18*, 1903-1908.